Available online at www.sciencedirect.com
ScienceDirect
Journal of Hazardous Materials 143 (2007) 41–48
Journal of Hazardous Materials
www.elsevier.com/locate/jhazmat

Phosphate removal using sludge from fuller's earth production

Yong Hee Moon [a], Jae Gon Kim [b], Joo Sung Ahn [b], Gyoo Ho Lee [b], Hi-Soo Moon [a,*]

[a] *Department of Earth System Sciences, Yonsei University, Seoul 120-749, South Korea*
[b] *Korea Institute of Geoscience and Mineral Resources, Daejon 305-350, South Korea*

Received 30 June 2005; received in revised form 5 July 2006; accepted 28 August 2006
Available online 1 September 2006

Abstract

This study assesses the phosphate removal capacity and mechanism of precipitation or adsorption from aqueous solutions in batch experiments by an industrial sludge containing gypsum ($CaSO_4{\cdot}2H_2O$) obtained as a by-product from a fuller's earth process.

The potential capacity for phosphate removal was tested using various solution concentrations, pH values, reaction times, and amount of sludge. The maximum phosphate adsorption capacity calculated using the Langmuir equation was 2.0 g kg^{-1}. The pH for the maximum adsorption by the sludge was neutral to alkaline (pH 7–12). Over 99% of phosphate was removed from a phosphate solution of 30 mg L^{-1} using 0.15 g of sludge in a 9-h reaction.

Sulfate (SO_4^{2-}) concentration increased with increasing initial phosphate concentration, possibly because of dissolution of gypsum and adsorption of both sulfate and phosphate. At high phosphate concentration (>1000 mg L^{-1}), relative constant concentration of Ca^{2+} was not consistent with adsorption of the most important phosphate removal mechanism. Results suggest that precipitation of calcium phosphate is principally responsible for phosphate removal under its high concentration. Agglomerated precipitate in the reaction sludge was observed by SEM and identified as brushite ($CaHPO_4{\cdot}2H_2O$) by XRD, FT-IR, and DTA. Based on thermodynamic considerations, it is suggested that the brushite will readily transform to more stable phases, such as hydroxyapatite ($Ca_5(PO_4)_3{\cdot}OH$).

Keywords: Adsorption; Brushite; Hydroxyapatite; Gypsum; Precipitation

1. Introduction

Phosphorus (P), an essential nutrient, is usually the growth-limiting factor of aquatic vegetation in surface waters. The critical level of this element that accelerates the growth of aquatic plants is 0.01 mg L^{-1} for dissolved P and 0.02 mg L^{-1} for total P [1]. Discharge of wastewater containing phosphates into surface water has long been an environmental concern since it can cause eutrophication of the receiving water body [2–4]. Several processes are currently applied for the removal of phosphate salts based upon their precipitation. In on-site wastewater treatment systems involve reaction with iron, aluminum and calcium compounds, such as the following [5–7].

$$Al_2(SO_4)_3{\cdot}14H_2O + 2PO_4^{3-} \leftrightarrow 2AlPO_4 + 3SO_4^{2-} + 14H_2O$$

$$FeCl_3 + PO_4^{3-} \leftrightarrow FePO_4 + 3Cl^-$$

$$CaCO_3 + H_3PO_4 \leftrightarrow CaHPO_4 + CO_2 + H_2O$$

Phosphate removal based on an adsorption mechanism has been tried with various materials, such as iron and calcium oxides [8], iron and aluminum oxides in spodosols [9], industrial products and synthetic compounds such as blast furnace slag [10] and synthetic iron oxide-gypsum compounds [11].

The major components of materials for phosphate removal are Al, Fe and Ca compounds. Phosphorus removal occurs through both adsorption and precipitation determined by redox potential and pH value [12–14]. Metal oxides are important PO_4^{3-} adsorption sites due to their multiple charged cation, high positive surface charge densities at near-neutral pH, and a propensity to hydroxylate in aqueous systems [15]. The reaction with calcium oxide, calcite or gypsum particle surfaces involves the adsorption of small amounts of phosphate followed by the precipitation of calcium phosphate. Initial adsorption is thought to occur at sites where lateral interaction with phosphate ions

* Corresponding author. Tel.: +82 2 2123 2669; fax: +82 2 392 6527.
E-mail addresses: yhmoon@yonsei.ac.kr (Y.H. Moon), hsmoon@yonsei.ac.kr (H.-S. Moon).

0304-3894/$ – see front matter © 2006 Elsevier B.V. All rights reserved.
doi:10.1016/j.jhazmat.2006.08.064

produces surface clusters that then act as nuclei for subsequent crystal growth. Such nuclei are presumably amorphous and are later transformed into crystalline calcium phosphate [7,16–19]. Precipitation of hydroxyapatite [HAP: $Ca_5(PO_4)_3{\cdot}OH$] is a process of great importance in various industrial processes ranging from water purification and fertilizer production to the fabrication of biocompatible ceramics [20,21]. In a biological context synthetic HAP has been extensively investigated as an analogous mineral to organically derived bones and teeth [22].

This study assessed the removal capacity of a sludge interacting with an aqueous solution with a relatively high phosphate concentration. The factors affecting adsorption and precipitation were investigated. The residue produced by the reaction was examined to verify the calcium phosphate phases.

2. Materials and methods

2.1. Material characterizations

During the activation process of bentonite, also called fuller's earth [23], highly acidic wastewater containing sulfuric acid is produced. When this liquid is neutralized with quicklime (CaO), a sludge is produced that mainly consists of gypsum ($CaSO_4{\cdot}H_2O$) and available metal oxides. A sludge sample was collected from a Korean fuller's earth production factory. The specimen was ground with an agate mortar and pestle to pass a 150 μm sieve. Grain size was determined using a laser particle size analyzer (Mastersizer 2000, Malvern Instruments Ltd.). The surface area of the sample was measured using the single-point Brunauer–Emmett–Teller (BET) method (Quantachrome, NOVA 2000 series). The bulk chemical composition of the sludge was derived through X-ray fluorescence (XRF, Shimadzu XRF-1700 Sequential). Solid phases of the sludge were variously examined using an X-ray diffractometer (XRD, Max-Science MXP-3 system), differential thermal analysis (DTA, Max-Science TG-DTA 2000S), a scanning electron microscope equipped with an energy dispersive X-ray system (SEM-EDX, JEOL JSM-5410-OXFORD ISIS 300), and infrared spectroscopy (IR, BrukerIFS 113V).

The XRD analyses were carried out upon finely powdered samples using a monochromator with Cu-$K\alpha_1$ radiation ($\lambda = 1.54060$ Å) at 5–50° in 2θ, a scan size of 0.02° and a scanning speed of $1^\circ\ min^{-1}$. DTA was performed with 50 mg powder samples heated at a rate of $10\ ^\circ C\ min^{-1}$. The IR analysis was carried out in the 4000–400 cm^{-1} spectral range using KBr pellets prepared with 4 mg samples and 200 mg of KBr. To confirm the possibility of heavy metal release, distilled deionized water (50 mL) was added to sludge samples (1 g) for 24 h and the resulting concentration of heavy metal in the solution was determined using a trace element analyzer (TEA, 3000 V, MTI Instruments PTY, Ltd.).

2.2. Experimental methods

The phosphate removal capacity test was performed as a four-batch experiment. The matrix solution was 0.01 M KCl, and a 10,000 mg L^{-1} phosphate stock solution was prepared using reagent grade KH_2PO_4. The batches were as follows: (1) 1.0 g of sludge with 50 mL of phosphate solutions ranging from 50 to 8000 mg L^{-1}, (2) 1.0 g of sludge with 50 mL of 2000 mg L^{-1} phosphate solution in a variety of pH conditions (3–13), (3) Several dosages of sludge ranging from 0.05 to 0.95 g with 50 mL of 30 mg L^{-1} phosphate solution. All suspensions remained overnight at room temperature, and (4) a kinetic series of experiments was performed by mixing 25 g of sludge and 5 L of 30 mg L^{-1} phosphate solution. Immediately after the end of the reaction period the pH was measured. Suspensions were filtered through 0.45 μm membrane filters. Filtrates were analyzed with a UV-Vis spectrophotometer (UV-160 PC, SHIMADZU) for PO_4^{3-} whilst using an ion chromatograph (IC, 350Alltech) to derive the concentration of SO_4^{2-}. The total cation concentration in the filtrates was determined via inductively coupled plasma-atomic emission spectrometry (ICP-AES, 138 Ultrace, Jobin Yvon) and TEA.

A thermodynamic calculation for the phosphate minerals presence was performed upon a computer program PHREEQC2 [24]. The equilibrium constants used are shown in Table 1. The saturation index of a mineral phase was defined as log(IAP/K) where IAP is the ion activity product, and K is the thermodynamic constant of equilibrium at a given temperature. The mineralogical change in the sludge after the phosphate removal tests was characterized by XRD, SEM-EDX, DTA, and IR techniques.

Table 1
Equilibrium constants of calcium and phosphate species at 25 °C used in the solubility calculations (after Lindsay [12])

Equilibrium reaction	$\log K_0$
Orthophosphoric acid	
$H_3PO_4 \leftrightarrow H^+ + H_2PO_4^-$	−2.15
$H_2PO_4 \leftrightarrow H^+ + HPO_4^{2-}$	−7.20
$HPO_4^{2-} \leftrightarrow H^+ + PO_4^{3-}$	−12.35
Mineral phases	
$CaSO_4{\cdot}2H_2O$ (gypsum) $\leftrightarrow Ca^{2+} + SO_4^{2-} + 2H_2O$	−4.64
$Ca(H_2PO_4)_2{\cdot}H_2O$ (MCP) $\leftrightarrow Ca^{2+} + 2H_2PO_4^- + H_2O$	−1.15
$CaHPO_4{\cdot}2H_2O$ (brushite) $+ H^+ \leftrightarrow Ca^{2+} + H_2PO_4^- + 2H_2O$	0.63
$Ca_4H(PO_4)_3{\cdot}2.5H_2O$ (octacalciumphosphate) $+ 5H^+ \leftrightarrow 4Ca^{2+} + 3H_2PO_4^{2-} + 2.5H_2O$	11.76
$Ca_5(PO_4)_3{\cdot}OH$ (hydroxyapatite) $+ 7H^+ \leftrightarrow 5Ca^{2+} + 3H_2PO_4^- + H_2O$	14.46

3. Result and discussion

3.1. Characteristics of sludge

Physical and chemical characteristics of the sludge material are given in Table 2. The surface area of the bulk sludge was a 46.16 $m^2\ g^{-1}$ with a mean particle diameter (d_{50}) of 15 μm. The sludge chemistry was dominated by calcium (20.67%), with significant amounts of aluminum and iron. XRD data show gypsum in a crystalline phase, which formed following the addition of CaO to sulfate-rich wastewater. Euhedral gypsum was also confirmed during SEM analysis. Aggregates of crystalline gypsum and amorphous Al and Fe compounds in the sludge were also identified by SEM-EDX. Fe and Al compounds were not detected during XRD analysis although a significant amount of Fe and Al oxide was apparent in the XRF analysis indicating that this was present as an amorphous compound phase. The batch test for heavy metal indicated slight alkalinity (pH 7.5) with a high concentration of dissolved Ca^{2+} and sulfate, presumably due to the dissolution of gypsum. The solubility of gypsum can be expressed as follows:

$$CaSO_4{\cdot}2H_2O \leftrightarrow Ca^{2+} + SO_4{}^{2-} + 2H_2O$$

The gypsum solubility product was calculated about 1.0 higher than the value of $\log K_0 = -4.6$ given by Lindsay [12]. Differences between the reference data and the result obtained in this experiment may be due to a release of sulfate from iron and aluminum compounds. Nevertheless, the concentrations of dissolved metals (Al, Fe, Pb, Zn, and Cd) were below the detection limits of the trace element analyzer (Table 2).

Table 2
Chemical and physical properties of the sludge used this study

Chemical composition (wt.%)	
SiO_2	3.24
Al_2O_3	10.68
TiO_2	0.08
Fe_2O_3	5.31
MgO	1.41
CaO	20.67
Na_2O	0.14
K_2O	0.1
MnO	0.09
P_2O_5	0.18
Batch test[a] concentration ($mg\ L^{-1}$)	
pH	7.5
Ca	578.0
Si	0.6
Al	<0.08[b]
Fe	<0.08
Mn	<0.03
Pb	<0.04
Zn	<0.04
Cd	<0.04
SO_4	1584
Physical properties	
Specific surface area ($m^2\ g^{-1}$)	46.16
Mean grain size (μm)	15 (d_{50})

[a] One gram of sludge: 50 mL deionized water, reacting for 24 h.
[b] Detection limit.

3.2. Phosphate removals by sludge

The most important parameters affecting the extent of phosphate removal were the initial concentration of phosphate, the amount of sludge, pH, and the reaction time [10]. The presence of Ca^{2+}, $PO_4{}^{3-}$ and $SO_4{}^{2-}$ with various phosphate concentrations, pH values, reaction times, and material dosage are plotted in Fig. 1. More than 90% of initial phosphate was removed from the solution at a relatively low concentration (<1000 $mg\ L^{-1}$, Fig. 1A), whereas the removal rate was less than 50% at a higher initial phosphate content (>5000 $mg\ L^{-1}$).

Phosphate may have been removed by adsorption, and/or by precipitation of any of several Ca phosphate compounds at relatively low concentration (<1000 $mg\ L^{-1}$). Sulfate concentration following gypsum solution increased gradually with increasing initial phosphate in the case of all samples. Higher phosphate concentrations (>1000 $mg\ L^{-1}$) however, indicated that the relative Ca^{2+} were not consistent with adsorption being the most important factor in the phosphate removal mechanism. The results suggest that precipitation of calcium phosphate was the principal mechanism for phosphate removal. Holtan et al. [25] and Johansson and Gustafsson [10] proposed that the mechanism of phosphate reaction with calcium sulfate varies from sorption (low phosphate concentration) to precipitation of calcium phosphate (higher concentration).

The phosphate can occur in a number of valance states but in natural water only +5 valances is significant. Dissolved phosphorus occurs as phosphoric acid (H_3PO_4) whereas H_2PO^{4-}, $HPO_4{}^{2-}$ and $PO_4{}^{3-}$ are dominant ions as its dissociation products. The proportion of each species in an aqueous solution is a function of pH. Below pH 7.2, $H_2PO_4{}^-$ is most abundant. Between pH 7.2 and 12, $HPO_4{}^{2-}$ is prevalent [26]. In the pH control batch test, the most effective pH range for phosphate extraction was from 7 to 12 showing more than 95% removal in the initial 2000 $mg\ L^{-1}$ solution (Fig. 1B). Consequently, the most effective phosphate phase for reaction between phosphorus ion varieties and sludge is indicated to be $HPO_4{}^{2-}$. A slight increase in the sulfate concentration under neutral to alkaline conditions could be related to the solubility of gypsum in the sludge. Adsorption of phosphate onto iron oxide generally decreases sharply with an increase of pH [27]. The opposite result in this experiment can be interpreted to be caused by a major component of calcium ions. According to the solubility product, a relatively neutral to alkali pH is required to cause precipitation of significant amounts of calcium phosphate. Higgins et al. [28] show in a lake remediation experiment that a high pH environment allows effective soluble phosphate removal by gypsum.

The effect of reaction time on the removal of phosphate by the sludge is shown in Fig. 1C. Equilibrium was achieved for 25 g of sludge mixed with 5 L of 30 $mg\ L^{-1}$ initial phosphate solution after about 9 h. The concentration of $SO_4{}^{2-}$ and Ca^{2+} and the pH level were relatively constant showing 2322 and 615 $mg\ L^{-1}$, respectively after equilibrium, until completion of a 119-h exper-

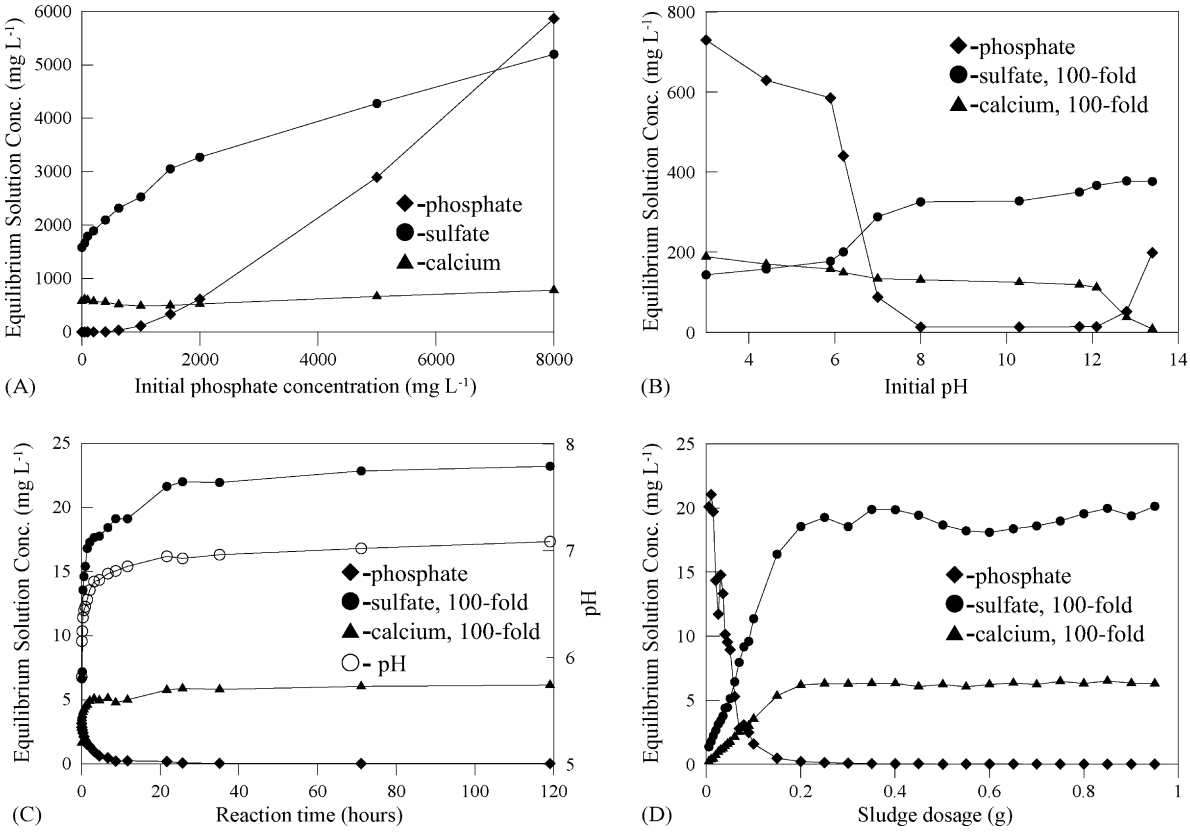

Fig. 1. Results of the bath and kinetic experiments: (A) 1.0 g of sludge with 50 mL of phosphate solution ranging from 50 to 8000 mg L^{-1}, (B) 50 mL of 2000 mg L^{-1} phosphate solution with 1.0 g of sludge at a variety of pH conditions (3–13), (C) 50 mL of 30 mg L^{-1} phosphate solution with several dosages of sludge ranging from 0.05 to 0.95 g and (D) reaction of 25 g of sludge and 5 L of 30 mg L^{-1} phosphate solution.

iment. The results of phosphate removal as a function of sludge dosage indicated that 0.15 g of sludge would be sufficient to treat 50 mL of 30 mg L^{-1} phosphate solution (Fig. 1D).

The Langmuir adsorption isotherm equation is able to describe the phosphate removal by the sludge:

$$\frac{C_e}{Q_e} = \frac{1}{bQ_o} + \frac{C_e}{Q_o}$$

where C_e is an equilibrium concentration (mg L^{-1}), q_e an amount adsorbed at equilibrium (mg kg^{-1}), and Q_o and b are isotherm constants. The maximum removal capacity calculated by the Langmuir isotherm equation is 2.0 g kg^{-1}, which is illustrated in Fig. 2.

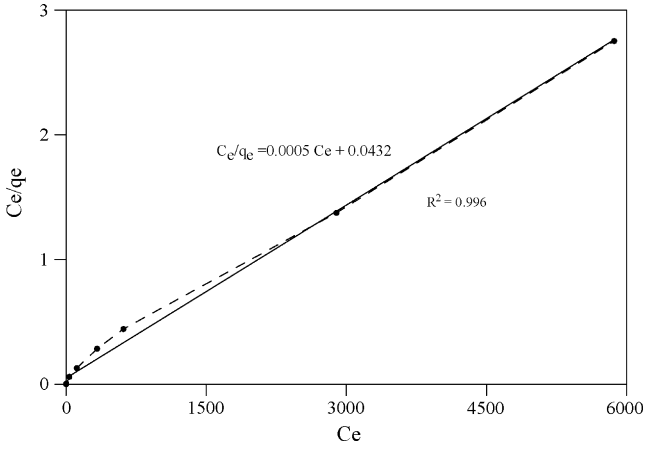

Fig. 2. Relationship between equilibrium solution phosphate (mg L^{-1}) and adsorbed phosphate (mg kg^{-1}) of the sludge from the bath experiment for various phosphate concentrations (C_e: equilibrium concentration (mg L^{-1}) and q_e: amount adsorbed phosphate concentration (mg kg^{-1})).

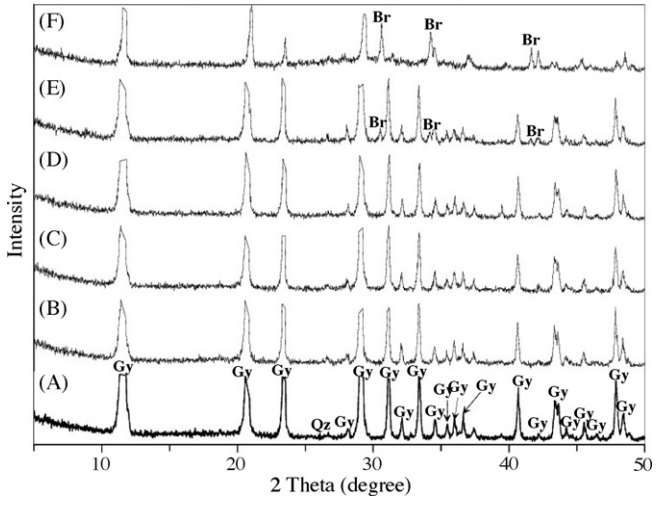

Fig. 3. X-ray diffraction patterns of the sludge obtained from the bath experiment for various phosphate concentrations: (A) from 0 mg L^{-1} initial reacting solution, (B) 400 mg L^{-1}, (C) 1000 mg L^{-1}, (D) 2000 mg L^{-1}, (E) 5000 mg L^{-1} and (F) 8000 mg L^{-1}. Gy: gypsum; Br: brushite; Qz: quartz.

3.3. Precipitated calcium phosphates

Following the XRD experiment Fig. 3A shows that the raw sludge is composed mainly of gypsum. Fig. 3B–D decrease in main peaks ($d = 7.61$, 3.80 and 3.07) intensity. After reaction with high phosphate concentrations of 5000 and 8000 mg L^{-1} (Fig. 3E and F), brushite (dicalciumphosphate; DCP, $CaHPO_4 \cdot 2H_2O$) peaks are notable. SEM analysis confirmed the presence of post reaction euhedral gypsum (Fig. 4A). Sludge treated with fewer than 1000 mg L^{-1} phosphate solution generated furrows on crystal surfaces (Fig. 4B and C). Agglomerated precipitates are abundantly evident in Fig. 4D. Sludge exposed to highly concentrated phosphate gave spherical precipitates (Fig. 4E and F). SEM-EDX results (Fig. 4) suggest

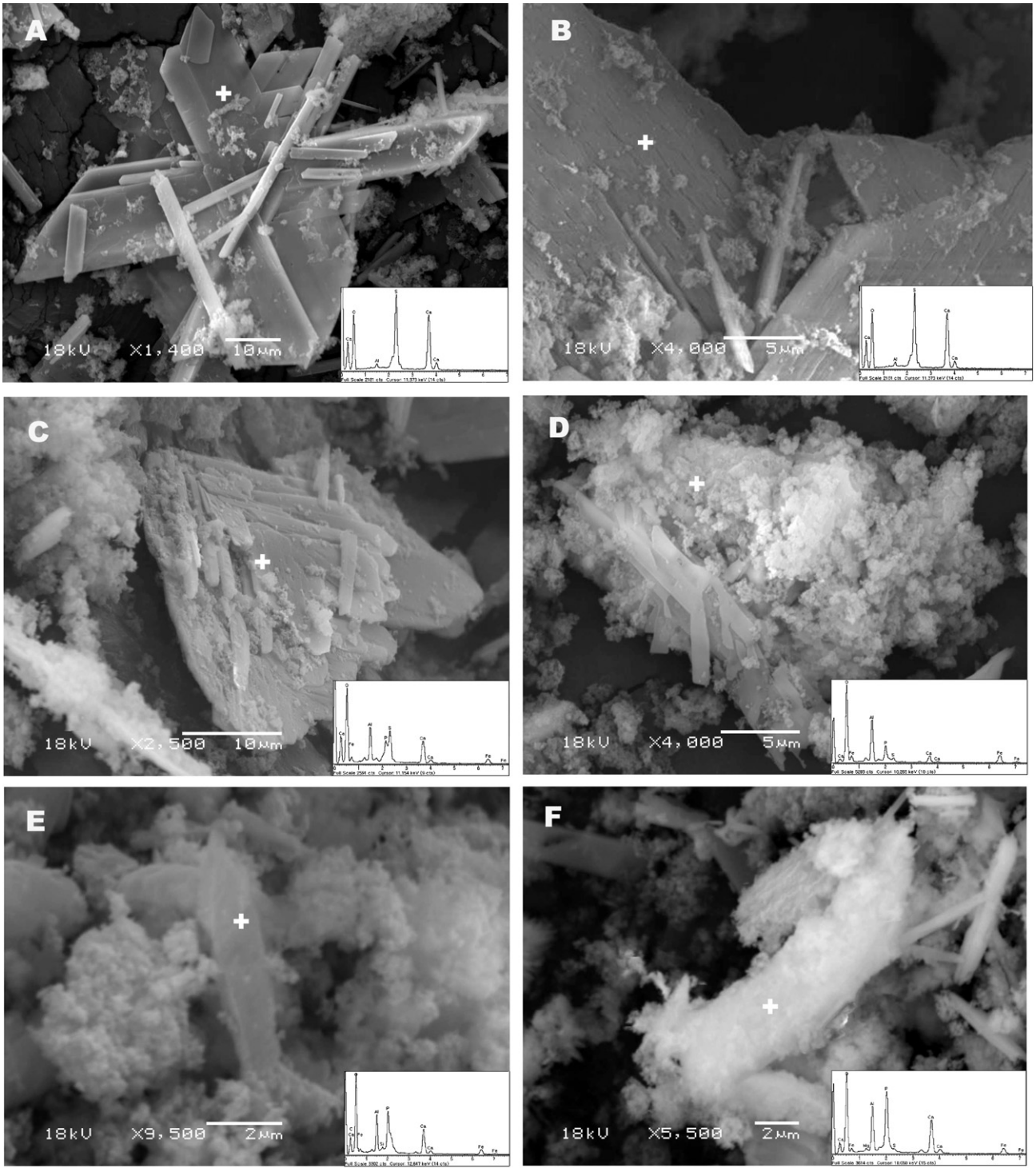

Fig. 4. Scanning electron micrographs and energy dispersive X-ray spectra of sludge obtained from the bath experiment for various phosphate concentrations: (A) from the 0 mg L^{-1} initial reacting solution, (B) 100 mg L^{-1}, (C) 400 mg L^{-1}, (D) 1000 mg L^{-1}, (E) 5000 mg L^{-1} and (F) 8000 mg L^{-1}. The symbol (+) is the EDX point.

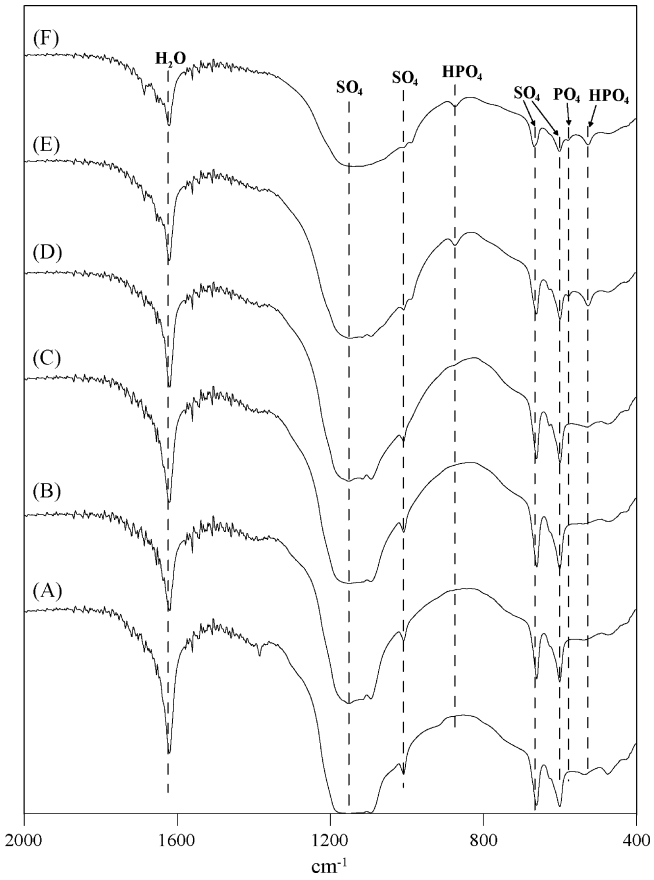

Fig. 5. Infrared spectra of the sludge obtained from the bath experiment for various phosphate concentrations: (A) from the 0 mg L^{-1} initial reacting solution, (B) 400 mg L^{-1}, (C) 1000 mg L^{-1}, (D) 2000 mg L^{-1}, (E) 5000 mg L^{-1} and (F) 8000 mg L^{-1}.

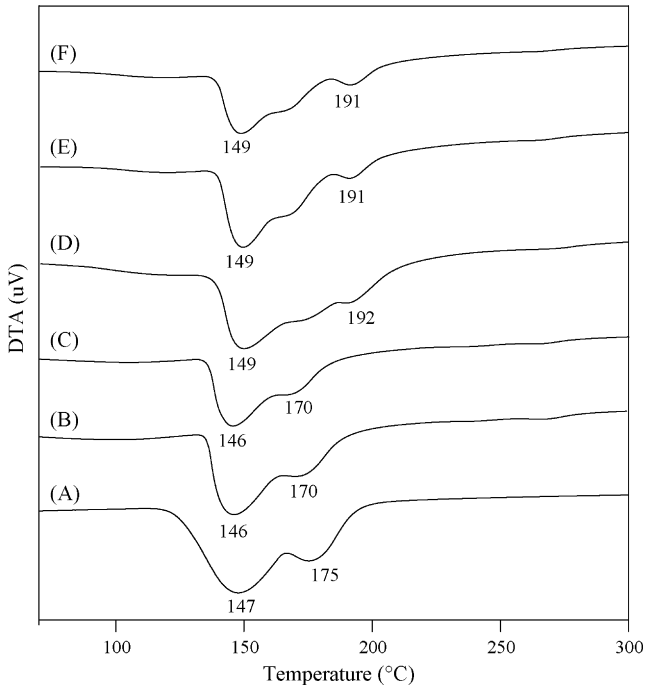

Fig. 6. Differential thermal analysis peaks of sludge obtained from the bath experiment for various phosphate concentrations: (A) from the 0 mg L^{-1} initial reacting solution, (B) 400 mg L^{-1}, (C) 1000 mg L^{-1}, (D) 2000 mg L^{-1}, (E) 5000 mg L^{-1} and (F) 8000 mg L^{-1}.

that there are particles of presumably amorphous calcium phosphate (ACP) slowly altering to a crystalline form depending on the absorbing surface condition. FT-IR absorption patterns are shown in Fig. 5. Low levels (<1000 mg L^{-1}) exhibit sulfate absorption bands only (Fig. 5A–C). Bands 526, 577 and 986 cm^{-1} for phosphate occur in addition to those for sulfate at 602, 668, and 1121 cm^{-1} for a higher phosphate concentration (Fig. 5D–F), thus confirming the presence of calcium phosphate phases [29].

Samples underwent thermal treatment in air, and the derived DTA curves were significantly different (Fig. 6). The endothermic peaks at 147 and 175 °C, of the raw (Fig. 6A) and reacted sludge (Fig. 6B and C) at low phosphate concentration (<1000 mg L^{-1}) can be ascribed to the dehydration of gypsum. On the other hand, the endothermic peaks at 149, 175 and 191 °C (Fig. 6D–F) with phosphate above 2000 mg L^{-1} may be related to the dehydration of DCP [30].

XRD, SEM-EDX, FT-IR, and DTA all suggest that an initial reaction occurred as adsorption by surface ligand exchange as a lateral interaction between phosphate ions and surface clusters producing a solid phase experiencing subsequent crystal growth. The solid phase is apparently amorphous calcium phosphate, which slowly transforms into crystalline calcium phosphate [31], variably dependent upon the adsorbing surface and solution pH. DCP is readily formed under acid conditions. Transformation to more basic calcium phosphate takes place at higher pH [7].

3.4. Calcium phosphate precipitation mechanism

Mineral equilibrium calculations are useful to predict reagents in the water system and in estimating their reactivity [32]. The Ca^{2+} and HPO_4^{2-} speciation data rules out the formation of ACP and/or octacalcium-phosphate (OCP, $Ca_4H(PO_4)_3{\cdot}2.5H_2O$) as the major phosphate removal mechanism. To investigate for any Ca–P precipitation the ion activity products (IAP) were calculated for different Ca–P phases using the PHREEQC2-speciated data [24]. The calculated saturation index values for calcium phosphate in the kinetic experiments are given in Table 3, and they show that the solution was saturated with HAP under most conditions.

In Fig. 7, the kinetic activity of $H_2PO_4^-$ or HPO_4^{2-} is plotted as a function of the pH. The solubility lines for calcium phosphate are drawn with Ca^{2+} being 10^{-2} in equilibrium solution. Fig. 7 can be used to estimate phosphate solubility relationships other than those used in its construction. The effect of different levels of Ca^{2+} can be obtained from the relationship:

$$\Delta\log(H_2PO_4^- \text{ or } HPO_4^{2-}) = \Delta\log Ca^{2+}\left(\frac{Ca}{P}\right)_i$$

where $(Ca/P)_i$ is the molar ratio of calcium to phosphorus in mineral (i) [12]. The solubility isotherms show the relationship to DCP, OCP, and HAP. The data points of the kinetic experiment appear to have three slopes in parallel to the DCP, OCP and

Table 3
Saturation indices of mineral phases calculated with PHREEQC2 for the kinetic experiment

Time (min)	Mineral phases		
	DCP[a]	OCP[b]	HAP[c]
1	0.44	N/A[d]	N/A
6	−1.13	N/A	0.07
11	−1.08	N/A	0.68
21	−1.10	N/A	0.97
36	−1.11	N/A	1.2
56	−1.14	N/A	1.29
86	−1.19	N/A	1.37
126	N/A	1.44	N/A
191	N/A	N/A	N/A
271	N/A	N/A	N/A
401	N/A	N/A	1.36
521	N/A	N/A	0.26
701	N/A	N/A	0.78
1301	N/A	N/A	1.08
1541	N/A	N/A	−0.49
2105	N/A	N/A	−0.89
4265	N/A	N/A	−0.94
7145	N/A	N/A	−1.11

[a] DCP: brushite ($CaHPO_4{\cdot}2H_2O$).
[b] OCP: octacalcium phosphate ($Ca_4H(PO_4)_3{\cdot}2.5H_2O$).
[c] HAP: hydroxyapatite ($Ca_5(PO_4)_3{\cdot}OH$).
[d] N/A: saturation index not calculated.

HAP, as the reaction proceeds. Although the data correspond to the undersaturation of DCP, the Ca phosphate phases tend to transform from DCP and OCP to HAP following reaction time (Fig. 7). This result is similar to the calculated saturation index values of the calcium phosphate phase in the kinetic experiment.

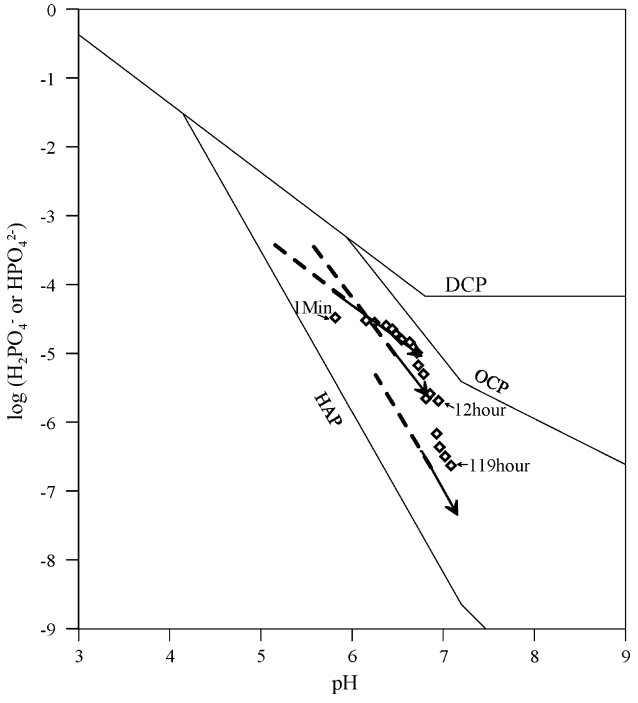

Fig. 7. A plot of pH vs. log($H_2PO_4^-$ or HPO_4^{2-}) from kinetic experiment data. The solubility lines of calcium phosphate are drawn with Ca^{2+} at 10^{-2} M in equilibrium solution [12]; DCP: brushite, OCP: octacalcium phosphate and HAP: hydroxyapatite.

Due to the prevalence of kinetic parameters over thermodynamic ones, the precipitate of the intermediate acidic solvated calcium phosphate phase is OCP in neutral solution. This serves as a template for the nucleation of more stable phases, accelerating the ACP–HAP conversion [7,17,18,20]. The nature of the complexes changes radically with a change in pH and the concentration of calcium or phosphate ions. In the pH region beyond the stability of acidic calcium phosphate, the overall kinetics are governed by reactions yielding to the formation of OCP growth units such as $H_2PO_4^-$ deprotonation and Ca^{2+} dehydration.

From the above results it can be inferred that although DCP and OCP are readily formed under acid or neutral conditions, they tend to transform to HAP at a higher pH.

4. Conclusions

The results in batch solution with a varying phosphate concentration showed that the maximum adsorption capacity calculated following the Langmuir adsorption isotherm was a phosphate removal capacity of 2.0 g kg^{-1}. The most effective pH range for phosphate removal was shown to be from 7 to 12. The reaction between phosphate solution and sludge apparently equilibrated after 9 h. 0.15 g of sludge is sufficient to remove 95% phosphate from 50 mL of 30 mg L^{-1} solution. Consequently, the sludge is a possible alternative as a filter material for the removal of phosphate from wastewater. This conclusion allows a determination of the efficiency of the process and the costs involved.

The phosphate removal mechanism at high phosphate concentration (>1000 mg L^{-1}) may involve the formation of calcium phosphate compounds rather than adsorption onto iron or aluminum oxide. In the reaction between various phosphate solution strengths and sludge, the harvested solid phases were identified by XRD, SEM-EDX, FT-IR, and DTA as brushite (dicalcium-phosphate, $CaHPO_4{\cdot}2H_2O$).

The solubility lines of calcium phosphates are described as a function of the pH and phosphate concentration. The kinetic experiment results are plotted as three slopes showing affinity to the solubility isotherms of brushite, octacalcium-phosphate (OCP, $Ca_4H(PO_4)_3{\cdot}2.5H_2O$), and hydroxyapatite (HAP, $Ca_5(PO_4)_3{\cdot}OH$). It is inferred that these form a template for the nucleation of more stable phases and accelerate an amorphous calcium phosphate to HAP conversion.

Acknowledgement

This work was supported by the Korea Research Foundation Grant (KRF-2005-015-C00465).

References

[1] T.C. Daniel, A.N. Sharpley, J.L. Lemunyon, Agricultural phosphorus and eutrophication: a symposium overview, J. Environ. Qual. 27 (1998) 251–257.
[2] A.N. Sharpley, S.C. Chapra, R. Wedepohl, J.T. Sims, T.C. Daniel, K. Reddy, Managing agricultural phosphorus for protection of surface waters. Issues and options, J. Environ. Qual. 23 (1994) 437–451.
[3] A.N. Sharpley, T.C. Daniel, J.T. Sims, D.H. Pote, Determining environmentally sound soil phosphorus levels, J. Soil Water Conserv. 51 (1996) 160–166.

[4] D.T. Van der Molen, A. Breeuwsma, P.C.M. Boers, Agricultural nutrient losses to surface water in the Netherlands. Impact, strategies and perspective, J. Environ. Qual. 27 (1998) 4–11.
[5] N.C. Brady, R.R. Weil (Eds.), The Nature and Properties of Soils, 12th ed., Prentice-Hall, New Jersey, 1999, pp. 540–584.
[6] Y. Avnimelech, Calcium-carbonate-phosphate surface complex in calcareous systems, Nature 288 (1980) 255–257.
[7] W.L. Lindsay, Phosphate mineral, in: J.B. Dixon, S.B. Weed (Eds.), Minerals in Soil Environments. No. 1 in SSSA Book Series, Soil Sci. Soc. Am. Madison, Winsconsin, 1989, pp. 1089–1130.
[8] M.J. Barker, D.W. Blowes, C.J. Ptacek, Laboratory development of permeable reactive mixtures for the removal of phosphorus from onsite wastewater disposal systems, Environ. Sci. Technol. 32 (1998) 2308–2316.
[9] G. Yuan, L.M. Lavkulich, Phosphate sorption in relation to extractable iron and aluminum in spodosols, Soil Sci. Soc. Am. J. 58 (1994) 343–346.
[10] L. Johansson, J.P. Gustafsson, Phosphate removal using blast furnace slags and opoka-mechanism, Water Res. 34 (2000) 259–265.
[11] O. Bastin, F. Janssens, J. Dufey, A. Peeters, Phosphate removal by a synthetic iron oxide-gypsum compound, Ecol. Eng. 12 (1999) 339–351.
[12] W.L. Lindsay, Phosphate. Chemical Equilibria in Soils, John Wiley & Sons, Inc., 1979, pp. 162–209.
[13] C.J. Richardson, Mechanisms controlling P retention capacity in fresh water wetlands, Science 228 (1985) 1424.
[14] S.P. Faulkner, B.C. Richardson, Physical and chemical characteristic of freshwater wetlands, in: D.A. Hammer (Ed.), Constructed Wetlands for Wastewater Treatment: Municipal, Industrial and Agricultural, Lewis Publishers, Chelsea, 1989, pp. 41–72.
[15] J.B. Michael, W.B. David, J.P. Carol, Laboratory development of permeable reactive mixtures for the removal of phosphorus from onsite wastewater disposal systems, Environ. Sci. Technol. 32 (1998) 2308–2316.
[16] F. Abbona, A.A. Baronnet, XRD and TEM study on the transformation of amorphous calcium phosphate in the presence of magnesium, J. Cryst. Growth 165 (1996) 98–105.
[17] J.L. Meyer, C.C. Weatherall, Amorphous to crystalline calcium phosphate phase transformation at elevated pH, J. Colloid Interf. Sci. 89 (1982) 257–267.
[18] M.R. Christoffersen, J. Christoffersen, W. Kibalczyc, Apparent solubilities of two amorphous calcium phosphates and of octacalcium phosphate in the temperature range 30–42 °C, J. Cryst. Growth 106 (1990) 349–354.
[19] S. Lazic, Microcrystalline hydroxyapatite formation from alkaline solutions, J. Cryst. Growth 147 (1995) 147–154.
[20] I. Joko, Phosphorus removal from wastewater by the crystallization method, Water Sci. Tech. 17 (1984) 121–132.
[21] P.W. Brown, M.J. Fulmer, Kinetics of hydroxyapatite formation at low temperature, J. Am. Ceram. Soc. 74 (1991) 934–940.
[22] W. Kibalczyc, M.R. Christoffersen, J. Christoffersen, A. Zielenkiewicz, W. Zielenkiewicz, The effect of magnesium ions on the precipitation of calcium phosphates, J. Cryst. Growth 106 (1990) 355–366.
[23] D.J. Morgan, Simultaneous DTA-ECA of minerals and natural mineral mixtures, J. Therm. Anal. 12 (1977) 245–263.
[24] D.L. Parkhurst, C.A.J. Appelo, User's Guide to PHREEQC2-A computer program for speciation, batch-reaction, one-dimensional transport, and inverse geochemical calculation, 1999.
[25] H. Holtan, L. Kamp-Nielsen, A.O. Stuanes, Phosphorus in soil, water and sediment: an overview, Hydrobiologia 170 (1988) 19–34.
[26] C.W. Fetter, Inorganic chemicals in ground water, in: Contaminant Hydrogeology, 2nd ed., Prentice Hall, Upper Saddle River, 1999, pp. 264–317.
[27] B.P.J. Hingston, A.M. Posner, J.P. Quirk, Anion adsorption by goethite and gibbsite. I. The role of the proton in determining adsorption envelopes, J. Soil Sci. 23 (1972) 177–191.
[28] B.P.J. Higgins, S.C. Mohleji, R.L. Irvine, Lake treatment with fly ash, lime, gypsum, J. WPCF 48 (1976) 2153–2164.
[29] E.E. Berry, C.B. Baddiel, The infra-red spectrum of dicalcium phosphate dihydrate (brushite), Spectrochim. Acta A 23 (1967) 2080–2097.
[30] R.C. Mackenzie, S. Caillere, The thermal characteristics of soil minerals and the use of these characteristics in the qualitative determination of clay minerals in soil, in: J.E. Gieseking (Ed.), Soil Components, vol. 2, Inorganic Components, Springer-Verlag, 1970, pp. 529–572.
[31] W. Stumn, J.O. Leckie, Phosphate exchange with sediments: its role in the productivity of surface water, in: Proceedings of the Fifth International Pollution Research Conference, San Francisco. Section III-26, 1970, pp. 1–9.
[32] W.J. Deutsch (Ed.), Groundwater Geochemistry: Fundamentals and Applications to Contamination, Lewis Publishers, New York, 1997, pp. 61–69.